A novel ErbB2 epitope targeted by human antitumor immunoagents

Fulvia Troise[1,2,*], Maria Monti[3,2,*], Antonello Merlino[4,5,*], Flora Cozzolino[3,2], Carmine Fedele[1], Irene Russo Krauss[4,5], Filomena Sica[4,5], Piero Pucci[2,3], Giuseppe D'Alessio[1] and Claudia De Lorenzo[1,2]

1 Dipartimento di Biologia Strutturale e Funzionale, Università di Napoli Federico II, Italy
2 CEINGE Biotecnologie avanzate, Napoli, Italy
3 Dipartimento di Chimica Organica e Biochimica, Università di Napoli Federico II, Italy
4 Dipartimento di Chimica, Università di Napoli Federico II, Italy
5 Istituto di Biostrutture e Bioimmagini, CNR, Naples, Italy

Two novel human antitumor immunoconjugates, engineered by fusion of a single-chain antibody fragment against human ErbB2 receptor, termed Erbicin, with either a human RNase or the Fc region of a human IgG$_1$, are selectively cytotoxic for ErbB2-positive cancer cells *in vitro* and *in vivo*. These Erbicin-derived immunoagents (EDIAs) do not show the most negative properties of Herceptin, the only humanized mAb against ErbB2 used in the therapy of breast carcinoma: cardiotoxicity and the inability to act on resistant tumors. These differences are probably attributable to the different ErbB2 epitopes recognized by EDIAs and Herceptin, respectively, as we have previously reported that they induce different signaling mechanisms that control tumor and cardiac cell viability. Thus, to accurately identify the novel epitope recognized by EDIAs, three independent and complementary methodologies were used. They gave coherent results, which are reported here: EDIAs bind to a different ErbB2 epitope than Herceptin and the other human/humanized antibodies against ErbB2 reported so far. The epitope has been successfully located in region 122–195 of extracellular domain I. These findings could lead to the identification of novel epitopes on ErbB2 that could be used as potential therapeutic targets to mitigate anti-ErbB2-associated cardiotoxicity and eventually overcome resistance.

Introduction

Overexpression of the ErbB2 tyrosine kinase receptor frequently occurs in breast cancer, and is associated with poor prognosis and with more aggressive clinical behavior [1,2]. Herceptin (trastuzumab), the only humanized antibody against ErbB2 in clinical use, has proven to be effective in the immunotherapy of breast carcinoma [3]. However, it can engender cardiotoxicity, and a high fraction of breast cancer patients are resistant to Herceptin treatment [4–6].

Two novel human antitumor immunoconjugates have been engineered in our laboratory by fusion of a single-chain antibody fragment (scFv) against human

Abbreviations

CDR, complementarity-determining region; ECD, extracellular domain of ErbB2 receptor; EDIA, Erbicin-derived immunoagent; ERB-hcAb, human compact antibody against ErbB2; ERB-hRNase, human anti-ErbB2 immunoRNase with Erbicin fused to human pancreatic RNase; HRP, horseradish peroxidase; PDB, Protein Data Bank; scFv, single-chain antibody fragment.

ErbB2, termed Erbicin [7], with either a human RNase or the Fc region of a human IgG$_1$, called Erb-hRNase and human compact antibody against ErbB2 (Erb-hcAb), respectively. Both immunoagents are selectively cytotoxic for ErbB2-positive cancer cells *in vitro* and *in vivo* [8–10].

Preliminary indirect findings have indicated that, on ErbB2-positive cells, Erbicin and its derived immuno-agents recognize an epitope different from that of Herceptin [11]. This led, on one hand, to the success of combined treatments *in vitro* of the Erbicin-derived immunoagents (EDIAs) with Herceptin [11], and on the other to the ascertainment of whether the EDIAs also presented the negative properties of Herceptin: cardiotoxicity and the inability to act on resistant tumors.

We found that Erb-hRNase and Erb-hcAb did not show cardiotoxic effects either *in vitro* on rat cardiomyocytes or *in vivo* on a mouse model, whereas Herceptin was strongly toxic [12]. This difference was found to be attributable to their different mechanisms of action, which can explain their different effects: Herceptin, unlike Erb-hcAb, induces apoptosis in cardiac cells. More interestingly, we found that EDIAs were active on Herceptin-resistant cells both *in vitro* and *in vivo* [13]. The sensitivity of these cells to treatment with EDIAs is probably attributable to the different epitope recognized by EDIAs [11], as Erb-hcAb, unlike Herceptin, was found to be capable of inhibiting the signaling pathway downstream of ErbB2 [13].

The critical role of the epitope recognized by antibodies against ErbB2 is further highlighted by the fact that pertuzumab, a new mAb against ErbB2 that is being tested in clinical trials, which recognizes an epitope distant from that of Herceptin (in the extracellular portion of ErbB2), acts with a different mechanism of action [14]. In fact, it sterically blocks the association of ErbB2 with other ErbB family members, and consequently prevents downstream receptor signaling.

The extracellular component of ErbB2 consists of four domains (domains I–IV). Cho *et al.* [15,16] described the crystal structure of the extracellular region of ErbB2 both free and in complex with Herceptin, and demonstrated that Herceptin binds the C-terminal end of domain IV [16], whereas the X-ray structure of the complex between ErbB2 and pertuzumab revealed that the latter binds to a different epitope, near the junction of domains I, II, and III [17].

Other mAbs against ErbB2 [18], such as N-12 and N-28, have been raised to different epitopes of ErbB2 and have been shown to induce opposing effects on tumor growth, thus suggesting that their differential biological activities can be attributed to the different receptor regions recognized.

A more complete definition of the ErbB2 epitope recognized by EDIAs has a dual relevance: first, to elucidate the relationship between the epitopes and signaling mechanisms that control tumor cell and cardiomyocyte viability, and second, to exploit the novel epitope as a potential therapeutic target to mitigate anti-ErbB2-associated cardiotoxicity and eventually overcome resistance.

With this aim, three complementary independent methodologies were used that gave coherent results: ELISA, MS, and combined homology modeling/computational docking. Altogether, the results obtained, and reported herein, strongly indicate that EDIAs bind to an ErbB2 epitope different from those of Herceptin and pertuzumab, and that this epitope is located in region 122–195 of domain I of the extracellular region of ErbB2.

Results

The epitope recognized by EDIAs is close to that of N-28

On the basis of previously reported results of ELISAs [11], all of the available mAbs against ErbB2, such as Herceptin (trastuzumab), 2c4 (pertuzumab), 7c2, and MAB74, recognize different epitopes from that of EDIAs.

The apparent binding affinity of Erb-hcAb for ErbB2 on SKBR3 cells, i.e. the concentration corresponding to half-maximal saturation, is about 1 nM, which is comparable to the value of 4 nM previously determined for the parental scFv (Erbicin) [8].

To determine whether the novel immunoagents recognize an epitope different from that targeted by N-28 [19], competition experiments were carried out by repeating the ELISAs on SKBR3 cells in the presence of N-28.

In these experiments the parental scFv (Erbicin) or Erb-hcAb was added at increasing concentrations (5–40 nM) to ErbB2-positive cells preincubated with N-28 at a saturating concentration (50 nM) for 1 h, or to untreated cells. Binding was detected with a peroxidase-conjugated mAb against His or against human Fc capable of revealing scFv or Erb-hcAb, respectively. As shown in Fig. 1, the presence of N-28 significantly inhibited the binding of the monovalent scFv Erbicin to the cells, whereas it slightly reduced the binding of the bivalent Erb-hcAb. This result can be easily explained by taking into consideration the higher avidity of binding to the cells of Erb-hcAb than of the parental scFv, as it has been previously reported [20] that binding of Erb-hcAb to ErbB2 is bivalent. The
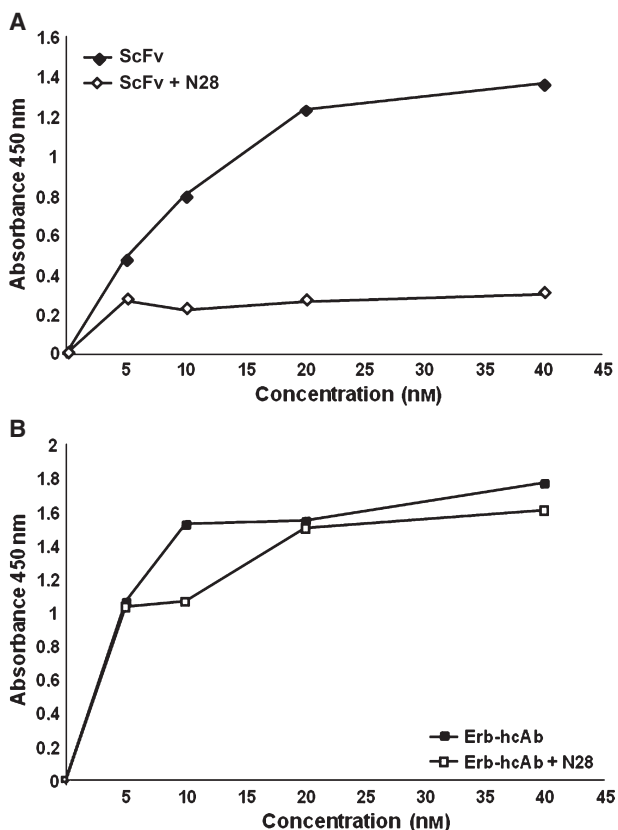
Fig. 1. Competitive ELISAs. Binding curves of Erbicin (A) and Erb-hcAb (B) for SKBR3 cells obtained by ELISAs performed in the absence (black symbols) or in the presence (empty symbols) of N-28. The values are reported as the mean of multiple independent experiments. Standard deviations were below 10%.

binding ability of N-28, detected with a secondary antibody (peroxidase-conjugated anti-mouse; data not shown), was unaffected by the presence of either Erbicin or Erb-hcAb. These results strongly suggest that the epitope recognized by the EDIAs is close to but does not overlap with that of N-28, as Erb-hcAb is still capable of binding to the cells in the presence of N-28, although with lower affinity.

Epitope mapping – ECD–Erb-hcAb complex

Two different strategies based on the integration of limited proteolysis experiments and MS methodologies were employed for the identification of the specific epitope on the extracellular domain of ErbB2 (ECD) recognized by Erb-hcAb. The first approach was based on the protection effect exerted by the antibody on the specific interacting region, which would prevent hydrolysis by proteolytic enzymes. ECD–Erb-hcAb was subjected to enzymatic digestion under strictly controlled

conditions to identify the protein region masked by the interaction.

ECD–Erb-hcAb was covalently bound to agarose beads and incubated with proteases under controlled time, enzyme/substrate ratio, temperature and pH conditions in order to maintain the stability of the complex and drive the hydrolysis towards the regions of the protein not involved in binding with the antibody. A sample of Erb-hcAb was also immobilized on the beads in the absence of ECD, and used as a control.

ECD–Erb-hcAb was initially digested with Glu-C endoprotease, with an enzyme/substrate ratio of 1 : 10 (w/w). Three aliquots of the digestion mixture were withdrawn at 30, 60 and 120 min, and the beads were separated from the supernatants by centrifugation. The beads, still containing the complex between Erb-hcAb and the ECD region involved in the interaction, were extensively washed, and the protein samples were eluted in denaturing conditions and fractionated by SDS/PAGE. The supernatants of the three aliquots were dried under vacuum, dissolved in Laemmli buffer, and used as a further control in the SDS/PAGE analysis.

Figure 2 shows the corresponding gel stained by colloidal Coomassie, where several bands belonging either to the antibody or to ECD were detected. A single specific protein band with an electrophoretic mobility of about 30 kDa could be observed in the three sample lanes; this band was absent in both controls. This
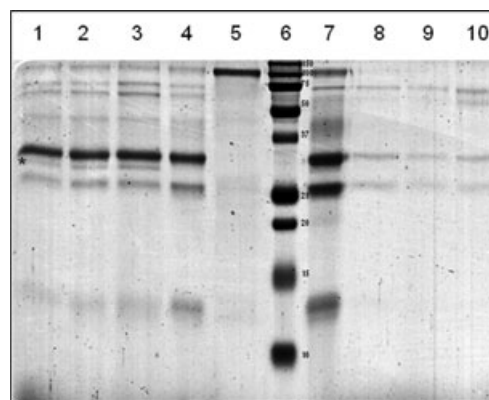

Fig. 2. Hydrolysis of ECD–Erb-hcAb by Glu-C. A single specific protein band at ~ 30 kDa, marked with the asterisk, is present in the three sample lanes and not in the controls. Lanes 1–3: beads with ECD–Erb-hcAb after 30, 60 and 120 min of incubation with Glu-C. Lane 4: beads with Erb-hcAb after 120 min of incubation with Glu-C (control). Lane 5: ECD at 0 min of incubation with Glu-C (control). Lane 6: markers. Lane 7: Supernatant from Erb-hcAb after 120 min of incubation with Glu-C (control). Lanes 8–10: Supernatant from ECD–Erb-hcAb after 30, 60 and 120 min of incubation with Glu-C.

result suggested that the 30-kDa protein band contained the ECD epitope specifically recognized by Erb-hcAb, protected from Glu-C digestion. The band was excised from the gel and digested *in situ* with trypsin, and the resulting peptide mixtures were analyzed by nanoLC-MS/MS.

A series of peptides mapping onto the N-terminal ECD domain and reported in Table 1 were unequivocally identified, suggesting that the epitope region was located within this region of the ECD structure. On the basis of the apparent molecular mass of the fragment as estimated by electrophoretic mobility, the enzyme specificity, and the arrangement of disulfide bridges in the ECD sequence, the occurrence of a single proteolytic event at Glu243 resulting in the production of fragment 1–243 was inferred. The difference in molecular mass from the expected mass value for this fragment, 26 763 Da, could be accounted for by the presence of several glycosylation sites localized in the N-terminal domain (Asn46, Asn102, Asn103, and Ans237). A second experiment, carried out with trypsin as a proteolytic probe, confirmed these results, as MS analyses led to the identification of the ECD region protected by the antibody in the N-terminal domain of the protein (Table 2).

Table 1. Experimental and theoretical masses of tryptic peptides obtained from *in situ* hydrolysis of the 30-kDa ECD fragment generated by the limited proteolysis experiment with Glu-C.

Peptide sequence	Amino acid position	MH+ theoretical	MH+ experimental
LPASPETHLDMLR	13–25	1479.76	1479.58
SLTEILK	122–128	803.48	803.61
NPQLCYQDTILWK	136–148	1678.82	1678.73
NNQLALTLIDTNR	154–166	1485.80	1485.77
GSRCWGESSEDCQSLTR	179–185	2014.83	2014.88

Table 2. Experimental and theoretical masses of tryptic peptides obtained from *in situ* hydrolysis of a specific 25-kDa ECD fragment generated by the limited proteolysis experiment with trypsin.

Peptide sequence	Amino acid position	MH+ theoretical	MH+ experimental
LPASPETHLDMLR	13–25	1479.76	1479.57
SLTEILK	122–128	803.48	803.35
DIFHKNNQLALTLIDTNR	149–168	2369.27	2368.94
NNQLALTLIDTNRSR	154–166	1485.80	1485.47
TVCAGGCARCK	196–206	1239.54	1239.52
CKGPLPTDCCHEQCAAGCTGPK	205–226	2504.02	2503.61

Limited proteolysis on isolated ECD

A complementary approach combining limited proteolysis on isolated ECD with western blot methodologies and protein identification by MS was further employed to confirm the above results and finely restrict the target epitope region.

Isolated ECD samples were incubated with Glu-C, with an enzyme/substrate ratio of 1 : 50, for 30 and 60 min respectively. A small aliquot corresponding to 10 μg of the initial protein content was withdrawn from each sample and fractionated by SDS/PAGE, together with the remaining portion of the 30-min and 60-min samples. The gel was divided, and the portion containing the small aliquots was used for western blot analysis with Erb-hcAb, whereas the remaining part of the gel was used for colloidal Coomassie staining.

The western blot analysis (Fig. 3) confirmed the presence of a large amount of undigested protein with an apparent molecular mass of 90 kDa (the theoretical molecular mass was 69 349 Da), given the presence of several glycosylation moieties. Besides the intact protein, a single band at 50 kDa was recognized by Erb-hcAb only in the 30-min sample. The corresponding band from the Coomassie-stained gel (Fig. 3) was excised and digested *in situ* with trypsin, and the resulting peptide mixture was analyzed by MALDI-TOF MS and LC-MS/MS. The ECD protein sequence was almost completely mapped from residues 11 to 347 (Fig. 3), confirming the occurrence of the epitope recognized by Erb-hcAb in the first two domains (L1 and CR1) of ECD.

In order to restrict the search for the epitope region, a second experiment was carried out with Glu-C, using a higher enzyme/substrate ratio (1 : 10) for 1 h. Samples were treated as described above. The western blot analysis of the fragments released by Glu-C hydrolysis showed the presence of a small amount of intact ECD and three immunopositive bands at 50, 30 and 24 kDa, respectively.

Mass mapping experiments carried out on the 50-kDa protein band excised from a preparative gel confirmed the above results indicating the occurrence of the immunoresponsive epitope within the first two ECD domains, L1 and CR1. Mass analyses of the peptides originating from the 30-kDa protein band showed almost complete sequence coverage of region 122–195 belonging to L1. Moreover, the absence of the N-terminal end in the mass spectra suggested that the epitope region would be limited to the C-terminal region of L1. The MS analyses of the tryptic peptides from the 24-kDa protein allowed for the identification of few peptides in region 122–166 of ECD, confirming
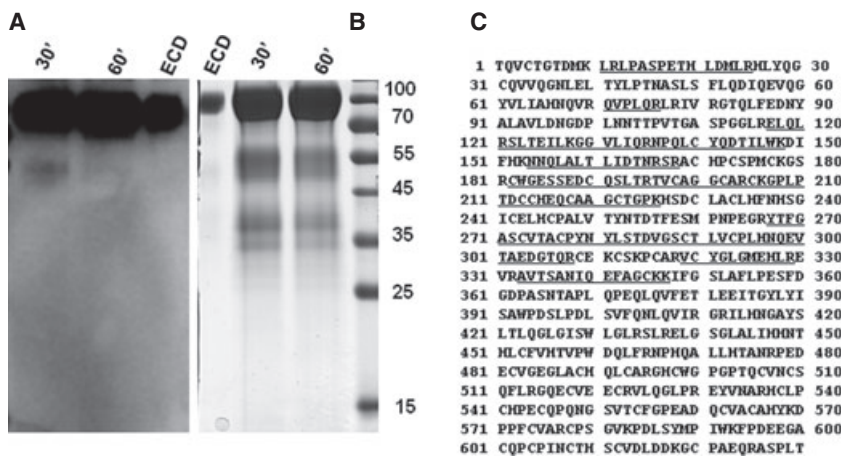
A **B**

C

```
  1 TQVCTGTDMK LRLPASPETH LDMLRHLYQG  30
 31 CQVVQGHLEL TYLPTNASLS FLQDIQEVQG  60
 61 YVLIAHNQVR QVPLQRLRIV RGTQLFEDNY  90
 91 ALAVLDNGDP LNNTTPVTGA SPGGLRELQL 120
121 RSLTEILKGG VLIQRNPQLC YQDTILWKDI 150
151 FHKNNQLALT LIDTNRSRAC HPCSPMCKGS 180
181 RCWGESSEDC QSLTRTVCAG GCARCKGPLP 210
211 TDCCHEQCAA GCTGPKHSDC LACLHFNHSG 240
241 ICELHCPALV TYNTDTFESM PNPEGRYTFG 270
271 ASCVTACPYN YLSTDVGSCT LVCPLHNQEV 300
301 TAEDGTQRCE KCSKPCARVC YGLGMEHLRE 330
331 VRAVTSANIQ EFAGCKKIFG SLAFLPESFD 360
361 GDPASHTAPL QPEQLQVFET LEEITGYLYI 390
391 SAWPDSLPDL SVFQNLQVIR GRILHNGAYS 420
421 LTLQGLGISW LGLRSLRELG SGLALIHHNT 450
451 HLCFVHTVPW DQLFRNPHQA LLHTANRPED 480
481 ECVGEGLACH QLCARGHCWG PGPTQCVNCS 510
511 QFLRGQECVE ECRVLQGLPR EYVNARHCLP 540
541 CHPECQPQNG SVTCFGPEAD QCVACAHYKD 570
571 PPFCVARCPS GVKPDLSYMP IWKFPDEEGA 600
601 CQPCPINCTH SCVDLDDKGC PAEQRASPLT
```

Fig. 3. Limited proteolysis of ECD with Glu-C and detection of the epitope-containing region by western blot. (A) Western blot with Erb-hcAb of fractions from limited proteolysis after 30 and 60 min; intact ECD was loaded as a control. (B) Colloidal Coomassie staining of fractions from limited proteolysis after 30 and 60 min; intact ECD was loaded as a control. (C) ECD sequence; the underlined sequence was identified by MALDI-TOF MS analysis in the protein band at 55 kDa from the 30-min Coomassie lane.
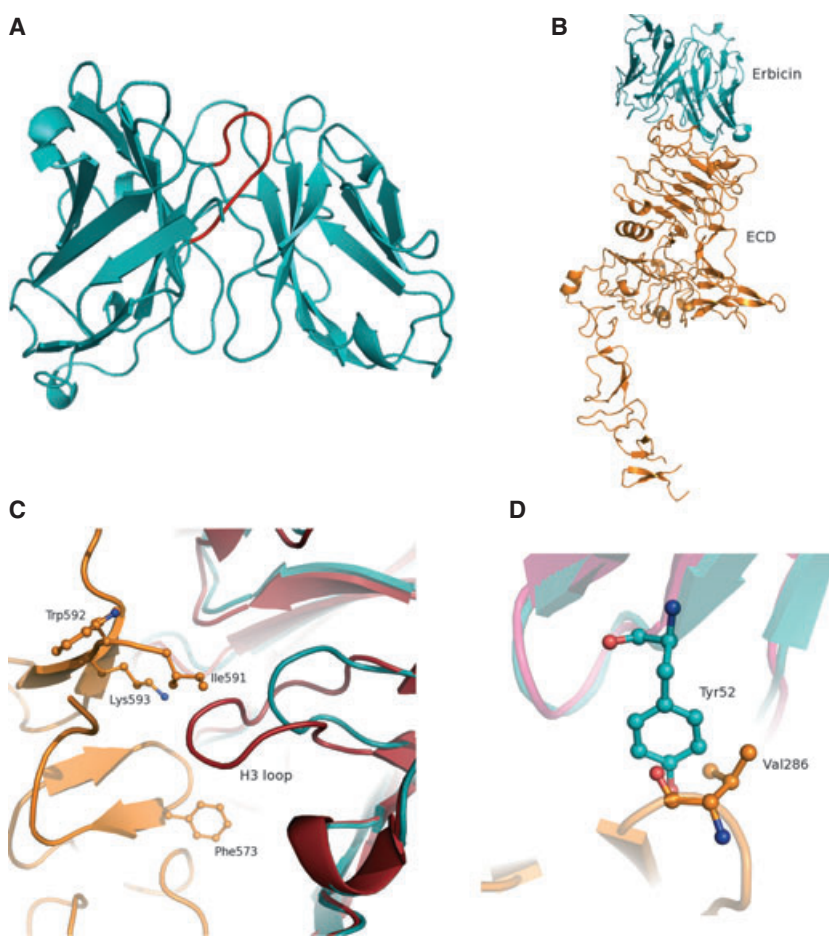

A **B**

C **D**

Fig. 4. (A) Ribbon diagram of a modeled structure of Erbicin. This and the following presentation were drawn with PYMOL (http://www.pymol.org) (B) Overall model of Erbicin (cyan) with ECD (orange) from computational docking. View of the interface region in the model of the Herceptin-like (C) or Pertuzumab-like (D) putative complex of Erbicin (cyan) with ECD (orange). The structures of Herceptin (red) and pertuzumab (pink) are also shown for comparison. As can be clearly seen from (D), the side chain of Tyr52 of Erbicin is spatially too close to the backbone atoms of ErbB2 Val286. Details of the docking calculation are described in Experimental procedures.

that the Erbicin-recognized epitope should lie within the C-terminal half of L1.

Investigation of Erbicin–ECD by computational docking

To reveal the molecular bases for the different binding properties of EDIAs with respect to the previously characterized antibodies, and to identify which interactions are responsible for EDIA–ErbB2 recognition, a homology modeling/computational docking approach was used. We first built a three-dimensional model of Erbicin, using the canonical structures method for the hypervariable loops [21–23] and standard homology modeling techniques for the framework regions. The model, reported in Fig. 4A, has a Prosa *Z*-score of

−6.53, a value in the range of scores typically found in proteins of similar sequence length, and shows that 96.4% of residues are in the most favored or in allowed regions of the Ramachandran map. The modeled protein is characterized by a predominantly canonical structure with a short (six residues) H3 loop. The molecular surface is rather flat, with cavities facing the complementarity-determining region (CDR) loops.

To identify the structural origins of the difference in binding properties between Erbicin and the two immunoagents of known structures, Herceptin and pertuzumab, we obtained two structural models of putative complexes between Erbicin and ECD. In particular, Erbicin was aligned with Herceptin (*C*-α rmsd = 0.94 Å) in the first complex (Herceptin-like) and with pertuzumab in the second complex (Pertuzumab-like) (*C*-α rmsd = 1.00 Å). These models provide valuable information on the origin of the different behavior of Erbicin with respect to Herceptin and pertuzumab. In particular, when compared to Herceptin, Erbicin presents a deletion in the H3 loop (six versus 11 residues) that prevents the binding to domain IV (Fig. 4). The origin of the differences between pertuzumab and Erbicin seems, instead, to be related to the replacement of Asp31, Asn52 and Asn54 by Ser31, Tyr52 and Gly54, respectively (see, for example, Fig. 4). It should be remembered that Asp31 of pertuzumab forms a strong hydrogen bond with the side chain of Ser288 of ECD and participates in hydrophobic interactions with the carbon atoms of Val286 and Thr290 of ECD. Furthermore, the ND2 atom of Asn52 forms a hydrogen bond with the backbone oxygen of Val286 of ECD, whereas the OD1 and ND2 atoms of Asn54 interact with the backbone atoms of Cys246 and Val286 and with the side chain atoms of Thr268.

To determine the region of ECD involved in the interaction with EDIAs, computational docking was performed with FTDOCK. These calculations were based on the model of Erbicin reported here, and evaluated in accordance with experimental evidence that the epitope involves ECD residues 122–195, on only domain I of ECD. The solutions were visually examined and evaluated with respect to experimental and theoretical criteria. In particular, the model should have a high surface complementarity at the interface and should bury a surface area of > 600 Å^2 per molecule. Finally, the model should have low energy and should be reproduced when docking calculations are repeated with different programs and/or input parameters. Upon clustering the 30 solutions with the lowest energy values, we identified three potential models, one of which fulfils the

previous criteria (Fig. 4). In this model, Erbicin binds ECD in the cleft between the light and the heavy chain variable domains. A total of 23 residues form the interface that is characterized by good surface complementarity (0.55). ECD–Erbicin buries about 750 Å^2 of accessible surface area per molecule over a long groove. The peptide regions of the antibody participating in direct contacts with ECD include the CDR H3 loop (Arg100, Asp101, and Ser102), the CDR H1 loop (Thr30, Ser31, and Tyr32), and Tyr181, Ser182, Gly225, Ser226, and Pro227. The ErbB2 residues at the interface mainly involve the Cys-rich fragment of region 162–190. In particular, Erbicin tightly binds the ECD region SRACHPCSPMCKGS(167–180), in which Cys173 forms an S–S bridge with Cys182, and Cys177 forms an S–S bridge with Cys190. A central role in the ECD–Erbicin interaction is played by His171 of ECD, which fills the antibody hydrophobic cavity lined by the side chains of Tyr123, Tyr163, Tyr164, Tyr181, and Ser182, where it may be involved in stacking interactions with one of the aromatic residues and in a hydrogen bond with the OG atom of the Ser.

Binding assays with specific peptides

In order to validate the ECD–Erbicin model, so that it could be used with confidence for further experimental and computational work, a peptide with the amino acid sequence SRASHPSSPHSKGS (ECD167–180) was synthesized and used for ELISAs with Erb-hcAb. In this peptide, Cys173 and Cys177 were replaced by Ser residues. As a control, parallel ELISAs were carried out with Herceptin.

As shown in Fig. 5, indirect ELISA revealed that Erb-hcAb was able to bind to SRASHPSSPMSKGS, although with a lower affinity than that previously measured for ECD [20], whereas Herceptin did not show any significant binding ability. The slight background binding of Herceptin to this peptide was similar to that observed when an unrelated peptide (RYPHCRYRGSPPSTRK) was used as a control (data not shown).

To assess the specificity of Erb-hcAb binding to sequence 167–180, competition ELISAs were performed. In these experiments, the ability of Erb-hcAb or Herceptin to bind to ECD was measured in the absence or in the presence of increasing concentrations of the soluble peptide mentioned above.

As shown in Fig. 6A, SRASHPSSPMSKGS inhibited the binding of Erb-hcAb to ECD, whereas it did not affect the binding of Herceptin to ECD (Fig. 6B).

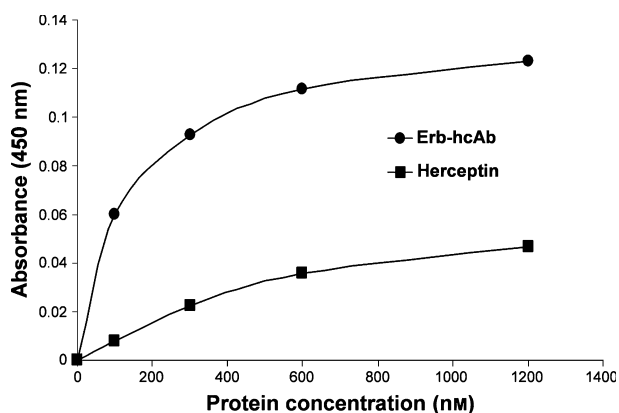To further test the validity of the model, a peptide containing the same sequence but with His171 replaced

Fig. 5. Binding assays with specific peptides of ErbB2. Binding curves of Erb-hcAb (black circles) and Herceptin (black squares) for ECD166–179 (SRASHPSSPMSKGS) obtained by ELISAs. The reported curves represent a summary of at least three determinations. Standard deviations were below 10%.

by Glu (SRASEPSSPMSKGS) was synthesized and tested as described above. Furthermore, an unrelated peptide (RYPHCRYRGSPPSTRK) was also used as a control in parallel experiments.

As shown in Fig. 6, neither the mutant or unrelated control peptide inhibited the binding of Erb-hcAb or Herceptin to ECD. Thus, these data provide further evidence that the epitope recognized by Erb-hcAb lies within region 122–195 of ErbB2 domain I.

The specific interaction between Erb-hcAb and SRASHPSSPHSKGS was also confirmed by fluorescence studies. Emission spectra of Erb-hcAb in the presence of this peptide and of its variant SRASEPSSPHSKGS were compared with those of the free antibody (data not shown). A variation in the signal intensity was observed only when the former peptide was added to Erb-hcAb.

Discussion

In previous reports, it has been already established that all EDIAs selectively bind to both ErbB2-positive cells and soluble purified ErbB2 antigen with apparent affinity values in the namomolar range, as determined by ELISA, surface plasmon resonance, and isothermal titration calorimetry [9,20].

The present study provides a significant indication at the molecular level of the interaction between ErbB2 and EDIAs by the identification and localization through epitope mapping of the antigenic peptide segment recognized by Erb-hcAb. The interactions of EDIAs with soluble ECD, the extracellular domain of ErbB2, was investigated through the use of three
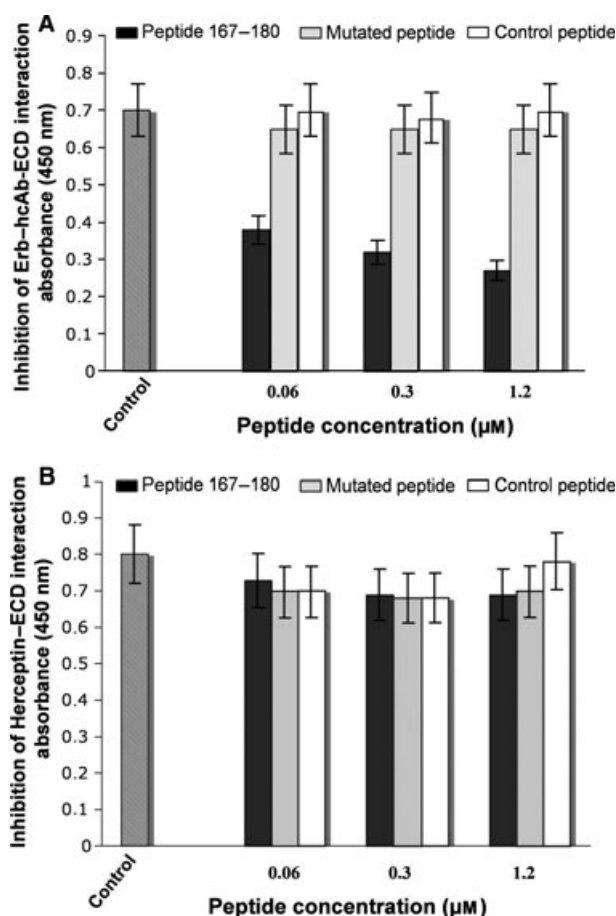

Fig. 6. Binding of Erb-hcAb and Herceptin to ECD in a competitive peptide ELISA. Erb-hcAb (A) and Herceptin (B) were preincubated with peptide 166–179 (black bars), the mutant peptide (striped bars), or control peptide (empty bars), and then tested for binding to immobilized ECD. As a control, Erb-hcAb or Herceptin was tested for binding to ECD in the absence of peptides.

independent complementary methodologies: ELISA, MS, and computational docking, which gave coherent results, thus providing, for the first time, accurate information on the epitope recognized by the EDIAs. Cell ELISAs with Erbicin, Erb-hcAb, and N-28, an antibody against ErbB2 that binds residues 216–235 of ECD [19], indicate that there is partial binding competition, suggesting that the epitope recognized by Erb-hcAb is close to the region recognized by N-28.

In a second approach, a combination of integrated MS and homology modeling/computational docking was used. The extracellular domain of ErbB2, already expressed and purified as a soluble recombinant protein [20], was complexed with Erb-hcAb previously immobilized on agarose beads. Digestion of the

antigen–antibody immobilized complex with suitable proteases was carried out, and the peptide(s) released from the antibody were analyzed by SDS/PAGE and sequenced by MALDI-TOF MS. The analyses led to the identification of a fragment bound to Erb-hcAb corresponding to region 1–243 of ECD. Furthermore, the digestion of the free antigen and western blotting analysis with Erb-hcAb confirmed the above mentioned results, and restricted the epitope location to segment 122–195. The docking calculations, performed on the basis of these findings, produced a model of the complex between Erbicin and ECD suggesting that EDIAs recognize an epitope comprising the region with the sequence SRACHPCSPMCKGS(167–180).

In the last approach, two peptides were designed and synthesized according to ECD sequence 167–180, and a mutant, in which His171, identified as one of the residues that could play a key role in the interaction, was replaced by Glu. In competition ELISA, the former peptide, unlike the mutant, was found to be capable of inhibiting the binding of Erb-hcAb to ECD.

Altogether, the results, validated through the use of three independent methodologies, indicate for the first time that EDIAs bind to a different ErbB2 epitope than Herceptin and the other human or humanized antibodies against ErbB2 reported so far. This epitope is located in region 122–195 of domain I of the extracellular region of ErbB2.

The definition of the ErbB2 epitope recognized by EDIAs could be of critical importance, given that EDIAs do not show the negative properties of Herceptin: cardiotoxicity and the inability to act on resistant tumors. These differences are probably attributable to the different ErbB2 epitopes recognized by EDIAs and Herceptin, as it has been reported that they induce different signaling mechanisms that control tumor and cardiac cell viability [12,13].

Thus, the localization of EDIAs' binding site could be useful not only to elucidate the relationship between the epitopes and signaling mechanisms that control tumor cell and cardiomyocyte viability, but also to exploit this epitope as a novel potential therapeutic target to mitigate anti-ErbB2-associated cardiotoxicity and eventually overcome resistance. Furthermore, the peptide corresponding to this novel epitope could be used in the future as a therapeutic vaccine. Finally, the definition of a new epitope is also important in view of the finding of the synergistic effects in combination therapy of two antibodies against two distinct epitopes of the same receptor [11,24,25] or epitopes on two different receptors, e.g. ErbB1 and ErbB2.

Experimental procedures

Antibodies and peptides

The antibodies used were: Herceptin (Roche, Basel, Switzerland), horseradish peroxidase (HRP)-conjugated antibody against His (Qiagen, Valencia, CA, USA), and HRP-conjugated goat anti-[human (affinity-isolated) IgG$_1$] (Fc-specific) (Sigma, St Louis, MO, USA). Erb-hcAb was prepared as previously described [9]. N-28 was a generous gift from M. Sela (Weizman Institute of Science, Rehovot, Israel).

The synthetic peptide corresponding to the amino acid sequence 167–180 (SRASHPSSPMSKGS) of ECD, the variant peptide with His171 replaced by Glu (SRA-**SE**PSSPMSKGS) and the unrelated control peptide (RYPHCRYRGSPPSTRK) were synthesized (95% purity) by Thinkpeptides, Oxford, UK. ECD was prepared as previously described [20].

ECD–Erb-hcAb

Aliquots of Erb-hcAb (800 µg) were immobilized on 0.4 mL of CNBr-activated Sepharose (GE Healtcare Amersham Bioscience AB, Uppsala, Sweden). The antibody was immobilized to the agarose via secondary amine chemistry, according to the manufacturer's instructions. Following blocking of the unreacted groups with 1 M ethanolamine hydrochloride (Sigma), the resin was washed with NaCl/P$_i$ (Sigma), and soluble ECD (400 µg) in NaCl/P$_i$ was added to the agarose containing the immobilized Erb-hcAb. Binding of the antigen was performed at 4 °C by gently rotating overnight.

Enzymatic hydrolyses on ECD–Erb-hcAb

Aliquots of 60 µL of agarose bead suspension containing 300 pmol of ECD complexed with Erb-hcAb were digested with Glu-C (Roche) or trypsin (Sigma), with an enzyme/substrate ratio of 1 : 10 (w/w), in a final volume of 120 µL of 10 mM Tris/HCl buffer (pH 7.4), at 37 °C. An equivalent amount of isolated antibody was digested in the same experimental conditions and used as a control.

Aliquots of 40 µL of sample and control were withdrawn after 30, 60 and 120 min of reaction, and centrifuged for 5 min at 400 *g* to remove the liquid phase containing unbound ECD fragments. The beads were then washed in Tris/HCl buffer, and the elution of antibody-bound ECD fragments was performed in Laemmli buffer (100 mM Tris/HCl, pH 6.8, 4% SDS, 0.2% Bromophenol Blue, 20% glycerol). Samples were fractionated on a 15% SDS/PAGE gel. The supernatant fractions containing the unbound proteins were dried under vacuum, dissolved in Laemmli buffer, and loaded onto the same gel as a further control. The gel was stained with Colloidal Coomassie (Pierce, Rockford, IL, USA).

Limited proteolysis on isolated ECD

An aliquot of 2 nmol ($\sim$ 140 μg) of ECD was digested with Glu-C, with two different enzyme/substrate ratios (1 : 50 and 1 : 10, w/w) in a final volume of 140 μL of 10 mM Tris/HCl buffer (pH 7.4) at 37 °C. Aliquots of 70 μL of the digestion mixture were withdrawn after 30 and 60 min, and the reactions were stopped by adding 23.6 μL of concentrated Laemmli buffer and boiling for 5 min. Small aliquots of 10 μg were withdrawn from each ECD sample and used for western blot assay. All samples were fractionated on the same gel (15% SDS/PAGE); the gel was then divided, and the part containing the small aliquots of protein was subjected to western blot analysis with 20 μg·mL^{-1} primary antibody (Erb-hcAb) in 1% nonfat milk in phosphate buffer (Sigma); the secondary antibody, HRP-conjugated anti-(human IgG$_1$) (Fc-specific), was used at a dilution of 1 : 1000 (v/v). The portion of the gel containing larger amounts of sample was stained with colloidal Coomassie, and employed for MS identification following in-gel tryptic hydrolysis.

In situ hydrolyses and MS analyses

Protein bands stained with colloidal Coomassie were excised from the gel and destained by repeated washing with 50 mM NH$_4$HCO$_3$ (pH 8.0) and acetonitrile. Samples were reduced and carboxyamidomethylated with 10 mM dithiothreitol (Sigma) and 55 mM iodoacetamide (Sigma) in 50 mM NH$_4$HCO$_3$ buffer (pH 8.0). Tryptic digestion of the alkylated samples was performed at 37 °C overnight, with 100 ng of trypsin.

For the MALDI-TOF MS analysis, 1 μL of peptide mixture was mixed with an equal volume of α-cyano-4-hydroxycynnamic acid as matrix [in acetonitrile/50 mM citric acid (70 : 30, v/v)], applied to the metallic sample plate, and air dried. The Applied Biosystems mass spectrometer was a MALDI Voyager DE-PRO equipped with a reflectron TOF analyser and used in delayed extraction mode. Mass calibration was performed by using the standard mixture provided by the manufacturer.

LC-MS/MS analyses were performed on a CHIP MS Ion Trap XCT Ultra equipped with a 1100 HPLC system and a chip cube (Agilent Technologies, Palo Alto, CA, USA). After loading, the peptide mixture (10 μL in 0.2% formic acid) was first concentrated and washed at 4 μL·min^{-1} in a 40-nL enrichment column (Agilent Technologies chip), with 0.1% formic acid as eluent. The sample was then fractionated on a C$_{18}$ reverse-phase capillary column (75 μm × 43 mm) onto a CHIP (Agilent Technologies chip) at a flow rate of 200 nL·min^{-1}, with a linear gradient of eluent B (0.2% formic acid in 95% acetonitrile) in A (0.2% formic acid in 2% acetonitrile) from 7% to 60% in 50 min. Peptide analysis was performed with data-dependent acquisition of one MS scan (mass range from 400 to 2000 *m/z*)

followed by MS/MS scans of the three most abundant ions in each MS scan.

ELISA

For assays of the binding of Erb-hcAb to ECD167–180 (SRASHPSSPMSKGS), a 96-well plate was coated with 20 μg·mL^{-1} of soluble peptide in NaCl/P$_i$, kept overnight at 4 °C, and blocked for 1 h at 37 °C with 5% BSA (Sigma) in NaCl/P$_i$. The plate was then rinsed with NaCl/P$_i$, and increasing concentrations of Erb-hcAb or Herceptin (25 nM to 1.2 μM) in ELISA buffer (NaCl/P$_i$/BSA 1%) were added and incubated for 2 h at room temperature with a blank control of NaCl/P$_i$. After rinsing with NaCl/P$_i$, HRP-conjugated anti-(human IgG$_1$) (Fc-specific) was added in ELISA buffer for antibody detection. After 1 h at room temperature, the plate was rinsed with NaCl/P$_i$, and bound antibodies were detected by using 3,3′,5,5-tetramethylbenzidine as substrate (Sigma). The product was measured at 450 nm with a microplate reader (Multilabel Counter Victor 3; Perkin Elmer, Cologno Monzese, Italy). The reported affinity values are the means of at least three determinations (standard deviations ≤ 10%).

The binding of Erbicin, Erb-hcAb and N-28 to the receptor was tested by using ErbB2-positive SKBR3 cells, as previously described [9]. For Erbicin detection, the peroxidase-conjugated mAb against His (Qiagen) was used; peroxidase-conjugated anti-(human IgG) (Fc-specific) (Sigma) and peroxidase-conjugated anti-(mouse IgG) (Pierce) were used for detection of human Erb-hcAb and mouse N-28, respectively.

Binding values were determined from the absorbance at 450 nm, and reported as the mean of at least three determinations (standard deviations ≤ 10%).

The ability of Erb-hcAb or Herceptin to bind to ECD was measured in the presence of increasing concentrations of three different soluble peptides: ECD167–180 (SRASHPSSPMSKGS), mutated ECD167–180 (SRA-SEPSSPMSKGS), and an unrelated control peptide (RYPHCRYRGSPPSTRK). A 96-well plate was coated with 5 μg·mL^{-1} purified ECD in NaCl/P$_i$ and left overnight at 4 °C. After blocking as described above, Erb-hcAb or Herceptin (50 nM) was added to the wells in triplicate before or after incubation with the peptides at increasing concentrations (60 nM–1.2 μM) overnight at 4 °C. After a 2-h incubation at room temperature, the plate was rinsed with NaCl/P$_i$, and bound Erb-hcAb or Herceptin was detected as mentioned above. Standard deviations were below 10%.

Computational techniques

The three-dimensional structure of Erbicin was built by homology modeling with the canonical structures method for the hypervariable loops [21–23] and standard homology modeling techniques for the framework regions. Briefly, the framework structure of the light and heavy chain variable

domains (V_L and V_H) from the Protein Data Bank (PDB) code 1DZB [26] was used as the scaffolding on which the six CDR loops were built. The CDR loops were assigned according to the definitions proposed by Chothia *et al.* [22,23], with the exception of the H3 CDR loop, which was predicted *de novo*. This is a short (six residues) loop, which should have a reduced conformational accessible space and only few conformations compatible with the rest of the protein structure. The Erbicin model was validated with PRO-CHECK [27], PROSA II [28], and CCP4 [29].

Rigid docking [30] of the Erbicin model onto ECD was performed with FTDOCK [31]. Given two molecules, FTDOCK computes the three-dimensional transformations of one of the molecules with respect to the other, with the goal of maximizing surface shape complementarity while minimizing the number of steric clashes. The scoring method of FTDOCK also includes electrostatic filters. The candidate models were then scored according to an energy function. The solutions were visually examined, clustered and evaluated with respect to experimental and theoretical criteria. The extensive rigid-body docking and the use of structural and biochemical data to filter the results is expected to produce a reasonable model of the complex. The final complex structure was then studied to analyze the intermolecular contacts and identify specific residue interactions between the proteins. This protocol allowed successful prediction of the structures of the ECD–pertuzumab and ECD–Herceptin complexes. A protein–protein interaction server was used to identify the residues at the interface in the complex and to evaluate the interface features [32]. The presence of putative hydrogen bonds and salt bridges was calculated with HBPLUS [33]. Assessment of the complex model with PRO-CHECK [27], PROSAII [28] and CCP4 [29] suggests that it has low energy, good stereochemical quality, and structural features of the interface including the surface complementarity value [34] that are comparable with those observed in the ECD–Herceptin (PDB code 1N8Z) and ECD–pertuzumab (PDB code 1S78) complexes.

Acknowledgements

References

1 Baselga J & Albanell J (2001) Mechanism of action of anti-HER2 monoclonal antibodies. *Ann Oncol* **12**(Suppl 1), S35–S41.

2 Slamon DJ, Clark GM, Wong SG, Levin WJ, Ullrich A & McGuire WL (1987) Human breast cancer: correlation of relapse and survival with amplification of the HER-2/neu oncogene. *Science* **235**, 177–182.

3 Stebbing J, Copson E & O'Reilly S (2000) Herceptin (trastuzumab) in advanced breast cancer. *Cancer Treat Rev* **26**, 287–290.

4 Sparano JA (2001) Cardiac toxicity of trastuzumab (Herceptin): implications for the design of adjuvant trials. *Semin Oncol* **28**, 20–27.

5 Cardoso F, Piccart MJ, Durbecq V & Di Leo A (2002) Resistance to trastuzumab: a necessary evil or a temporary challenge? *Clin Breast Cancer* **3**, 247–257. discussion 258–249.

6 De Lorenzo C & D'Alessio G (2008) From immunotoxins to immunoRNases. *Curr Pharm Biotechnol* **9**, 210–214.

7 De Lorenzo C, Palmer DB, Piccoli R, Ritter MA & D'Alessio G (2002) A new human antitumor immunoreagent specific for ErbB2. *Clin Cancer Res* **8**, 1710–1719.

8 De Lorenzo C, Arciello A, Cozzolino R, Palmer DB, Laccetti P, Piccoli R & D'Alessio G (2004) A fully human antitumor immunoRNase selective for ErbB-2-positive carcinomas. *Cancer Res* **64**, 4870–4874.

9 De Lorenzo C, Tedesco A, Terrazzano G, Cozzolino R, Laccetti P, Piccoli R & D'Alessio G (2004) A human, compact, fully functional anti-ErbB2 antibody as a novel antitumour agent. *Br J Cancer* **91**, 1200–1204.

10 De Lorenzo C, Cozzolino R, Carpentieri A, Pucci P, Laccetti P & D'Alessio G (2005) Biological properties of a human compact anti-ErbB2 antibody. *Carcinogenesis* **26**, 1890–1895.

11 De Lorenzo C, Troise F, Cafaro V & D'Alessio G (2007) Combinatorial experimental protocols for Erbicin-derived immunoagents and Herceptin. *Br J Cancer* **97**, 1354–1360.

12 Riccio G, Esposito G, Leoncini E, Contu R, Condorelli G, Chiariello M, Laccetti P, Hrelia S, D'Alessio G & De Lorenzo C (2009) Cardiotoxic effects, or lack thereof, of anti-ErbB2 immunoagents. *FASEB J* **23**, 3171–3178.

13 Gelardi T, Damiano V, Rosa R, Bianco R, Cozzolino R, Tortora G, Laccetti P, D'Alessio G & De Lorenzo C (2010) Two novel human anti-ErbB2 immunoagents are active on trastuzumab-resistant tumours. *Br J Cancer* **102**, 513–519.

14 Badache A & Hynes NE (2004) A new therapeutic antibody masks ErbB2 to its partners. *Cancer Cell* **5**, 299–301.

15 Cho HS & Leahy DJ (2002) Structure of the extracellular region of HER3 reveals an interdomain tether. *Science* **297**, 1330–1333.

16 Cho HS, Mason K, Ramyar KX, Stanley AM, Gabelli SB, Denney DW Jr & Leahy DJ (2003) Structure of the

extracellular region of HER2 alone and in complex with the Herceptin Fab. *Nature* **421**, 756–760.

17 Franklin MC, Carey KD, Vajdos FF, Leahy DJ, de Vos AM & Sliwkowski MX (2004) Insights into ErbB signaling from the structure of the ErbB2–pertuzumab complex. *Cancer Cell* **5**, 317–328.

18 Stancovski I, Hurwitz E, Leitner O, Ullrich A, Yarden Y & Sela M (1991) Mechanistic aspects of the opposing effects of monoclonal antibodies to the ERBB2 receptor on tumor growth. *Proc Natl Acad Sci USA* **88**, 8691–8695.

19 Yip YL, Novotny J, Edwards M & Ward RL (2003) Structural analysis of the ErbB-2 receptor using monoclonal antibodies: implications for receptor signalling. *Int J Cancer* **104**, 303–309.

20 Troise F, Cafaro V, Giancola C, D'Alessio G & De Lorenzo C (2008) Differential binding of human immunoagents and Herceptin to the ErbB2 receptor. *FEBS J* **275**, 4967–4979.

21 Al-Lazikani B, Lesk AM & Chothia C (1997) Standard conformations for the canonical structures of immunoglobulins. *J Mol Biol* **273**, 927–948.

22 Chothia C & Lesk AM (1987) Canonical structures for the hypervariable regions of immunoglobulins. *J Mol Biol* **196**, 901–917.

23 Chothia C, Lesk AM, Tramontano A, Levitt M, Smith-Gill SJ, Air G, Sheriff S, Padlan EA, Davies D, Tulip WR *et al.* (1989) Conformations of immunoglobulin hypervariable regions. *Nature* **342**, 877–883.

24 Ben-Kasus T, Schechter B, Lavi S, Yarden Y & Sela M (2009) Persistent elimination of ErbB-2/HER2-overexpressing tumors using combinations of monoclonal antibodies: relevance of receptor endocytosis. *Proc Natl Acad Sci USA* **106**, 3294–3299.

25 Friedman LM, Rinon A, Schechter B, Lyass L, Lavi S, Bacus SS, Sela M & Yarden Y (2005) Synergistic down-regulation of receptor tyrosine kinases by combinations of mAbs: implications for cancer immunotherapy. *Proc Natl Acad Sci USA* **102**, 1915–1920.

26 Ay J, Keitel T, Kuttner G, Wessner H, Scholz C, Hahn M & Hohne W (2000) Crystal structure of a phage library-derived single-chain Fv fragment complexed with turkey egg-white lysozyme at 2.0 A resolution. *J Mol Biol* **301**, 239–246.

27 Laskowski RA, Moss DS & Thornton JM (1993) Main-chain bond lengths and bond angles in protein structures. *J Mol Biol* **231**, 1049–1067.

28 Sippl MJ (1993) Recognition of errors in three-dimensional structures of proteins. *Proteins* **17**, 355–362.

29 Collaborative Computational Project no. 4 (1994) The CCP4 suite: programs for protein crystallography. *Acta Crystallogr* **50**, 760–763.

30 van Dijk AD, Boelens R & Bonvin AM (2005) Data-driven docking for the study of biomolecular complexes. *FEBS J* **272**, 293–312.

31 Gabb HA, Jackson RM & Sternberg MJ (1997) Modelling protein docking using shape complementarity, electrostatics and biochemical information. *J Mol Biol* **272**, 106–120.

32 Reynolds C, Damerell D & Jones S (2009) ProtorP: a protein–protein interaction analysis server. *Bioinformatics* **25**, 413–414.

33 McDonald IK & Thornton JM (1994) Satisfying hydrogen bonding potential in proteins. *J Mol Biol* **238**, 777–793.

34 Lawrence MC & Colman PM (1993) Shape complementarity at protein/protein interfaces. *J Mol Biol* **234**, 946–950.